Monte Carlo Simulation of Many-Chain Star Polymer Solutions

Luis A. Molina and Juan J. Freire*

Departamento de Química Física, Facultad de Ciencias Químicas, Universidad, Complutense, 28040 Madrid, Spain

Received May 7, 1998; Revised Manuscript Received October 16, 1998

ABSTRACT: Many-chain systems of star polymer molecules in a good solvent have been investigated using a dynamic Monte Carlo algorithm on a simple cubic lattice. Several bead−jump moves are proposed for the central part of stars with three and four arms, in addition to the usual combination of bends, crankshafts, and terminal moves also employed for linear chains. Static properties such as the chain size, or the mean square radius of gyration, are calculated. It is shown that the ratio of the star size to that of a linear chain with the same number of units does not change with concentration. The collective scattering functions are also obtained for different concentrations, and the interchain structure factors obtained from these functions are compared with those corresponding to linear chains. The dynamics generated from the Monte Carlo trajectories yields Rouse modes which exhibit the expected dependencies on the mode number and chain length. Finally, the elastic and rotational relaxation modes of individual chains are shown to obey dependencies on the arm length and the number of arms that are compatible with the predictions of scaling theory.

Introduction

Flexible star polymer chains having different numbers of arms, *f*, can currently be prepared through the use of modern synthesis methods. The conformational properties of these chains are significantly different from those of homologous linear chains, due to the great influence of the central part of the chain, where the density of polymer beads is very different from that in the outer parts.[1] Scaling[2] and renormalization group[3] theories have been applied to the description of some of properties. Numerical simulation is an alternative to explore more involved properties and verify the theoretical predictions.

Although many investigations have examined the behavior of single star chains, simulation studies of many-chain systems are scarce.[4] Monte Carlo simulations on a lattice are particularly efficient to explore many-chain systems of linear chains.[5,6] In the case of stars, however, new rules must be incorporated in the Monte Carlo algorithms with fixed bonds to allow for changes in the central unit position. Up to now, these modifications have only been introduced for stars with three arms.[7,8]

Scaling theory[2] predicts that the size, e.g. the mean square radius of gyration $\langle S^2 \rangle$, of a single star chain immersed in a good solvent (excluded volume conditions) scales with the total number of units N in a way similar to a linear chain under the same conditions

$$\langle S^2 \rangle^{1/2} \approx N^{\nu} \tag{1}$$

where ν is a critical exponent, whose value has been calculated[9] to be $\nu = 0.588$. The ratio g of the size of a branched (star) chain to that of a linear chain with the same N, i.e.

$$g = \langle S^2 \rangle_{br} / \langle S^2 \rangle_{l} \tag{2}$$

can be used to characterize the branching architecture. Applying Gaussian statistics for the intramolecular distances between units, i.e., ignoring excluded volume or any other type of intramolecular interactions, leads to an analytical formula for the ratio g for ideal chains:

$$g = (3f - 2)/f^2 \tag{3}$$

Renormalization group considerations have lead to the conclusion that eq 3 is also valid for chains in excluded volume conditions.[3] This conclusion has been verified through experimental measurements and single-chain numerical simulations. However, g is greater for single chains at the Θ point due to the influence of three-body effects in the central region of the star, or core, which causes an expansion of the arms within this region. Then, the ratio g is greater for star chains in the Θ state than for ideal chains.[1,3] Moreover, it is known that the excluded-volume effects are screened out for chains in melts or in concentrated solutions.[9,10] It is not clear, however, if the radius of gyration of the star (and the ratio g) in these systems should be similar to that of chains in the Θ state or to ideal chains.

Also according to the scaling theory,[2] a semidilute solution of star chains behaves as a semidilute solution of linear chains, though it also contains regions of starlike coronas corresponding to the chain cores.[1] The crossover from the dilute to the semidilute regimes occurs at $\Phi \cong \Phi^*$ (Φ is the polymer volume fraction) where Φ^* is the overlapping concentration that can be estimated as

$$\Phi \cong N/(4\pi \langle S^2 \rangle^{3/2}/3) \tag{4}$$

(assuming that $\langle S^2 \rangle$ is expressed in reduced units, relative to the length of a single unit). At the overlapping concentration, we expect a qualitative change in the osmotic pressure. This effect corresponds to a compensation of the difference in local polymer concentration in the star core with respect to the rest of the solution.[11] The osmotic pressure discontinuity leads to a peak in the region $x = q^2 \langle S^2 \rangle \approx 1$ (**q** is the scattering vector) region of the scattering intensity that indicates a global ordering at the distance range equal to the mean size of a chain. The peak is more noticeable for stars with higher numbers of arms.

10.1021/ma980722z CCC: $18.00
Published on Web 12/29/1998

In a star chain, one can consider the relaxation time of the global chain shape, τ_e, obtained from the time-correlation function of the center-to-arm's end distance. τ_e is clearly conditioned by the interactions in the star core. This relaxation time is distinguishable from the rotational relaxation, τ_D, which defines the time required for the star to rotate or translate a distance approximately equal to its size. τ_D should be nearly independent of core effects. The scaling theory predicts that for a single chain in a good solvent[1,2]

$$\tau_e \approx N_a^{1+2\nu} f^{(1-2\nu)/2} \tag{5}$$

i.e. τ_e is nearly independent of the number of arms for chains with the same number of units per arm, $N_a = N/f$. However, τ_D is predicted to behave as

$$\tau_D \approx N_a^{1+2\nu} f^{2-\nu} \tag{6}$$

Equation 5 has been verified through Monte Carlo calculations performed with the bond fluctuation model[12,13] and through Brownian dynamics simulations.[14] Up to the present, however, the rotational mode has not been characterized as a single exponential through any simulation procedure.[1]

In the present work, we have performed Monte Carlo simulations of many-chain star systems on a simple cubic lattice. We consider two different types of functionalities $f = 3$, 4. Our algorithm includes specific rules for the moves of the central beads in these types of chains. A methodological aim has been to verify that these rules lead to a correct description of the Rouse mode behavior, as has been previously shown for the well-established rules in linear chains.[5,6] Moreover, we have investigated the problems outlined above. Thus, we have computed the chain size and ratio g as a function of concentration. Also, we have computed the collective scattering of the systems and analyzed their x or q dependence. Finally, the relaxation times τ_e and τ_D have been obtained for single chains and the results are compared with the scaling theory prediction.

Monte Carlo Algorithm and Numerical Methods

We consider n star chains whose units are placed on a simple cubic lattice of side L. (The distance between neighboring sites is taken as the length unit). Units of the same or different chains cannot occupy the same site (single occupancy rule). This condition gives rise to excluded volume or good solvent conditions in dilute systems. The polymer volume fraction is, therefore, $\Phi = nN/L^3$. Periodic boundary conditions are established, and an adequately large value of L is adopted to avoid interactions of a chain with its own image, $L \geq 2N^{1/2} + 5$, according to the criterion established for linear chains (this condition is more strict for stars having the same number of units, whose sizes are smaller). All these specifications are detailed in previous work for linear chains.[15]

Configurational changes are introduced by randomly choosing a polymer unit. According to its position, the following different jump-moves are considered.

(a) Inner Moves. If the unit is a inner bead placed between two perpendicular bonds, a kink−jump, involving these two bonds is attempted, and the unit moves to the site at the opposite corner of the square partially defined by these two bonds if this site is not occupied by a contiguous unit. Otherwise, we try a three-bond crankshaft, involving also the unit connecting the chosen bead to the occupied site. These moves are shown in Figure 1.

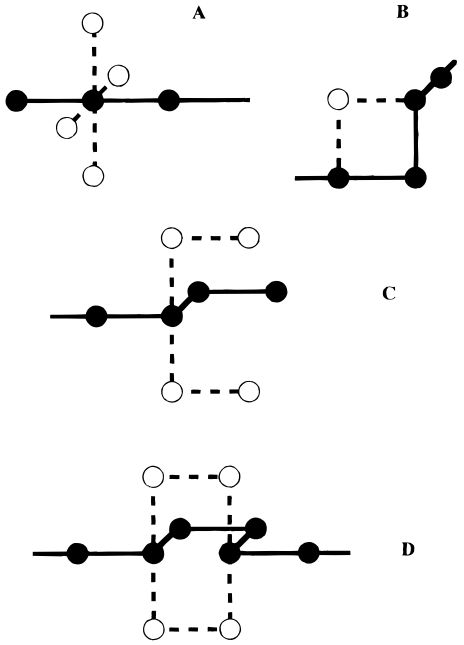

Figure 1. Terminal and inner moves: (a) terminal kink−jump; (b) inner kink−jump; (c) terminal crankshaft; (d) inner crankshaft.

(b) Terminal Moves. If the unit is at the end of an arm, a move is attempted to place the last bond in a direction perpendicular to its previous position. If the unit is bonded to an arm end and it is placed between perpendicular bonds, we choose between performing an inner kink−jump or changing these terminal bonds simultaneously to perpendicular positions. The two types of terminal moves can respectively be considered as "broken" kink−jumps or crankshafts. Figure 1 also illustrates the terminal moves.

(c) Central Unit Moves. We introduce specific rules to move the central unit of the star, which, otherwise, is considered identical to the rest. (Of course, real star polymer molecules might possess heavy core-monomers.) The rules are strongly conditioned by the functionality of the central unit. The different types of attempted moves are illustrated in Figure 2. For $f = 3$ we consider a move where the first bonds in two arm perform a kink−jump, while the first and second bonds in the remaining arm execute a crankshaft. This move was previously used by Sikorski et al.[7,8] Another possibility consists of carrying out a "double crankshaft" involving simultaneously the first two bonds of two arms, which also bends the first bond of the third arm to a perpendicular position. In the case of stars with four arms, we consider a kink−jump involving the first two bonds in two arms. The first two bonds in the remaining arm can perform a "double crankshaft" or, alternatively, are involved in two simultaneous crankshafts in perpendicular directions which align the first bonds of these two arms. Since these more complex moves can only be attempted for very specific dispositions of units in the central region, we favor the occurrence of these configurations by performing an inner move of a randomly chosen contiguous unit (first bead of an arm) when a central bead move it is not possible. We have verified that this alternative moves do not affect to the results for the dynamic properties

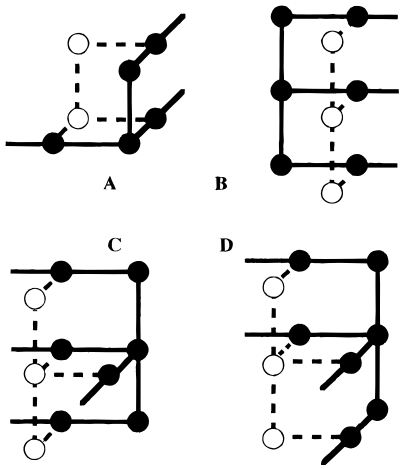

Figure 2. Central unit moves: (a) $f = 3$, kink−jump and crankshaft; (b) $f = 3$ double crankshaft; (c) $f = 4$, kink−jump and double crankshaft; (d) $f = 4$, kink−jump and two perpendicular crankshafts.

while significantly increases the acceptance rates of the central unit moves.

From the dynamic point of view all these moves are considered to be similar, independently of the number of bonds implied, following the specifications previously used for linear chains.[5,6] (Reptation moves cannot be defined for the stars, and they are not used for the generation of Monte Carlo trajectories in linear chains in order to avoid a biased dynamics.) A Monte Carlo step, which is adopted as the time unit in the simulations, is defined to correspond to nN moves so that all the units have had a single opportunity to be chosen for one of these bead−jump attempts.

The initial configuration is obtained by randomly choosing n sites on the lattice that correspond to the initial positions of the different star central units. New bonds are randomly added to the different chain arms complying with the single occupancy rule up to the point where all the arms have N_a units. Configurational changes according to the prescribed moves are performed simultaneously with the growth of the chains in order to favor the equilibration of the system. This equilibration process is particularly costly for nondilute star solutions that cannot easily interpenetrate due to the presence of the central cores. (Equivalent algorithms for linear chains may use the alternative and very efficient reptation moves for equilibration purposes, though reptations are never considered in the generation of the dynamic trajectories.) The equilibration is subsequently completed after the chains are fully grown. Typically, we allow for 3×10^5 equilibration Monte Carlo steps. A similar number of steps are used for the calculation of properties.

Results and Discussion

(a) Chain Size and Shape. Tables 2−4 contain a summary of the results for linear and star chains ($f = 3$ and $f = 4$) that directly depend on the mean quadratic intramolecular distances. We have evaluated $\langle S^2 \rangle$

$$\langle S^2 \rangle = (1/N^2) \sum_i^N \sum_j^N \langle R_{ij}^2 \rangle \qquad (7)$$

(where $\langle R_{ij}^2 \rangle$ are the mean-quadratic intramolecular distances) for linear and star chains for chains of different number of units per arms in the range $N_a = 12-100$. Polymer volume fractions vary between $\Phi = 0$ (single chain) and $\Phi = 0.3$. The critical overlapping concentrations, based in eq 4 and the radii of gyration of the chains in dilute solution are included in Table 1. It can be observed that the finite values of Φ used in the simulations correspond to the dilute regime for the smallest chains but they are beyond Φ^* for the longest chains. log−log fits of the results to eq 1 yield the numerical values of exponent ν_N shown in Tables 2−4. It can be observed that the numerical results for ν_N for dilute solutions are in good agreement with the theoretical value corresponding to the critical exponent in excluded volume conditions, $\nu = 0.588$. When concentration increases, ν_N decreases since the excluded volume effects are screened out. (For an ideal chain, $\nu = {}^1/_2$). The rate of decrease does not depend noticeably of the chain functionality. In Figures 3 and 4, we show representations of $\langle S^2 \rangle / N^{2\nu}$ vs $N_a^{-1/2}$ for the different types of chains in the dilute and most concentrated systems,[16] using the theoretical values of ν, $\nu = 0.588$

Table 1. Overlapping Concentration Φ^* for the Different Chains Estimated from Equation 4 and the Radius of Gyration at Dilute Solution

	f		
N_a	2	3	4
12	0.27	0.29	0.33
16	0.22	0.24	0.26
24	0.15	0.17	0.19
32	0.12	0.13	0.16
50	0.089	0.096	0.11
100	0.052	0.057	0.063

Table 2. Size and Shape Related Quantities ($f = 2$)

	ν_N	$\langle A \rangle$
theory	0.5;[a] 0.588[b]	0.526[c]
Θ chain	0.5[a]	0.518[d]
single chain	0.602	0.556
$\Phi = 0.1$	0.561	0.525
$\Phi = 0.2$	0.561	0.550
$\Phi = 0.3$	0.544	0.539

[a] Ideal chain. [b] Excluded volume. [c] Equation 3 (ideal chain). [d] Reference 20, Monte Carlo calculations.

Table 3. Size and Shape Related Quantities ($f = 3$)

	ν_N	g	$\langle A \rangle$
theory	0.5;[a] 0.588[b]	0.78[c]	0.361[d]
Θ chain	0.5[a]	0.81−0.83[e]	
single chain	0.581	0.75	0.345
$\Phi = 0.1$	0.583	0.76	0.353
$\Phi = 0.2$	0.551	0.78	0.339
$\Phi = 0.3$	0.530	0.78	0.327

[a] Ideal chain. [b] Excluded volume. [c] Equation 3 (ideal chains). [d] Equation 9 (ideal chains). [e] Monte Carlo simulations discussed in ref 3.

Table 4. Size and Shape Related Quantities ($f = 4$)

	ν_N	g	$\langle A \rangle$
theory	0.5;[a] 0.588[b]	0.62[c]	0.273[d]
Θ chain	0.5[a]	0.66−0.68[e]	0.273[f]
single chain	0.593	0.61	0.243
$\Phi = 0.1$	0.572	0.63	0.249
$\Phi = 0.2$	0.563	0.62	0.250
$\Phi = 0.3$	0.532	0.61	0.240

[a] Ideal chain. [b] Excluded volume. [c] Equation 3. [d] Equation 9. [e] Monte Carlo simulations discussed in ref 3. [f] Reference 20, Monte Carlo calculations.

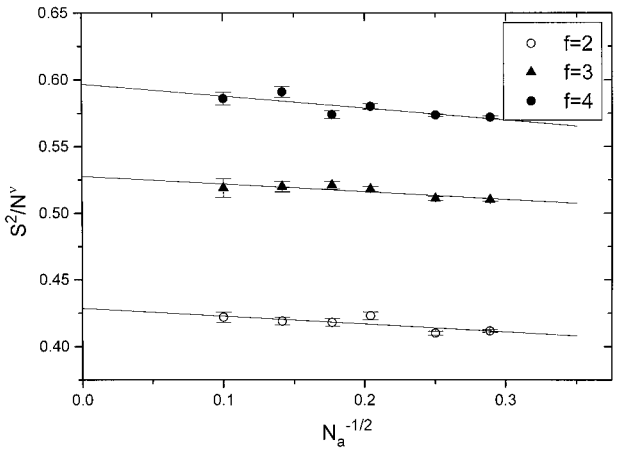

Figure 3. $\langle S^2\rangle/N^{2\nu}$ ($\nu = 0.588$) vs $N_a^{-1/2}$ for linear and star chains in dilute solutions.

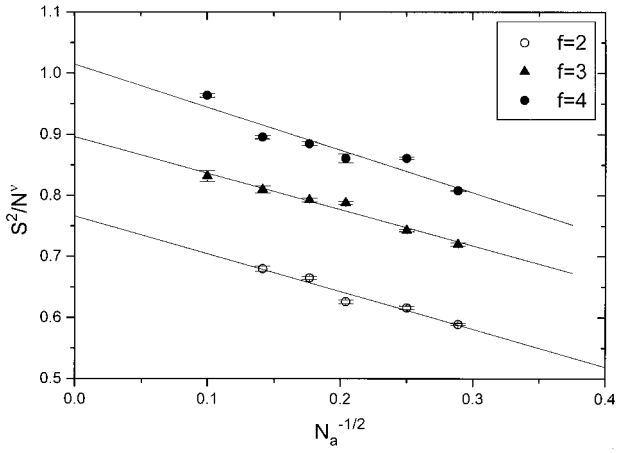

Figure 4. $\langle S^2\rangle/N^{2\nu}$ ($\nu = 0.5$) vs $N_a^{-1/2}$ for linear and star chains, $\Phi = 0.3$.

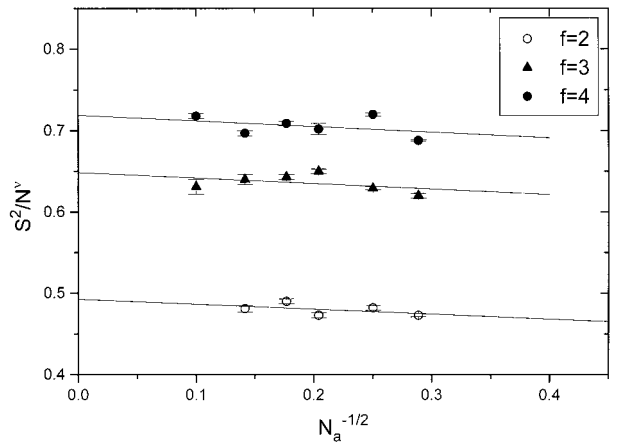

Figure 5. $\langle S^2\rangle/N^{2\nu}$ (ν is the corresponding fitted ν_N in Tables 2−4) vs $N_a^{-1/2}$ for linear and star chains, $\Phi = 0.3$.

or $\nu = 0.5$. It is observed that the dilute chains obey the expected behavior, exhibiting a slight linear dependence with $N_a^{-1/2}$. The chains in concentrated systems, however, show considerably more pronounced dependencies on N_a, as it can be expected from the noticeable difference between the fitted values of ν_N and $\nu = 0.5$. In Figure 5, we show the corresponding plots for the concentrated systems obtained by substituting $\nu = 0.5$ by the fitted ν_N. These plots are very similar to those obtained for the dilute systems. This shows that the excluded volume is only partially screened out for our highest concentration, since the investigated values of Φ are always close to the overlapping concentration or lower than Φ^*.

Consistent with the linear variations of $\langle S^2\rangle/N^{2\nu}$ vs $N_a^{-1/2}$ we have performed extrapolations of the results for ratio g, defined by eq 2, to the long chain limit. They are also included in Tables 3 and 4. Ratios g are maintained approximately constant for all the different concentrations and always very close to the theoretical prediction in the absence of intramolecular interactions. According to the renormalization group theory, the excluded volume contributions for linear and branched chains cancel out in first-order perturbation calculations.[3] Our Monte Carlo results show that the screening out of excluded volume due to an increase in concentration depends weakly on the chain architecture. It should be noted, however, that the ratio g corresponding to chains in the Θ state (obtained through previous Monte Carlo simulations) are noticeably higher than the ideal prediction, due to the arm stretching in the central part of the star.[1,3] The conclusion is, consequently, that the radius of gyration of stars in a Θ solvent should be greater than that in the melt state. This conclusion is also supported by the different numerical values of the radius of gyration obtained from neutron scattering data.[1]

Moreover, we have evaluated the chain asphericity, characterized by the ratio

$$\langle A\rangle = \frac{\langle \sum_i^3 \sum_j^3 (\lambda_i - \lambda_j)^2 \rangle}{4\langle (\sum_i^3 \lambda_i)^2 \rangle} \qquad (8)$$

where the eigenvalues λ_k are obtained through the numerical diagonalization of the 3×3 tensor of quadratic components of the radius of gyration. The long chain extrapolations for the asphericity ratios are also included in Tables 2−4. Obviously, a higher number of arms favor more spherical shapes (i.e. smaller values of $\langle A\rangle$). The results for star chains are slightly higher than the theoretical prediction[17]

$$\langle A\rangle = \frac{10(15 - 14/f)/f}{15(3 - 2/f)^2 + 4(15 - 14/f)/f} \qquad (9)$$

valid only for ideal chains (i.e. for chains without intramolecular interactions). The presence of excluded volume effects seem to favor a more spherical shape for the stars, a result opposite to the trend observed for linear chains. This feature has been also observed in previous simulations for single chains.[18,19] The present results for nondilute systems indicate that the asphericities of linear chains suffer a small but noticeable change when concentration increases, and the results for the nondilute systems are generally closer to the theoretical limit for ideal chains. However, the shapes of star chains are practically constant in the explored range of concentrations. In fact, they are always similar to those obtained with excluded volume conditions. These ratios are noticeably smaller than the ideal chain values obtained from eq 9 or the Monte Carlo values previously calculated for single chains in the Θ state.[20]

(b) Collective Scattering Factor. The collective static scattering function of the system $S(q)$ has been

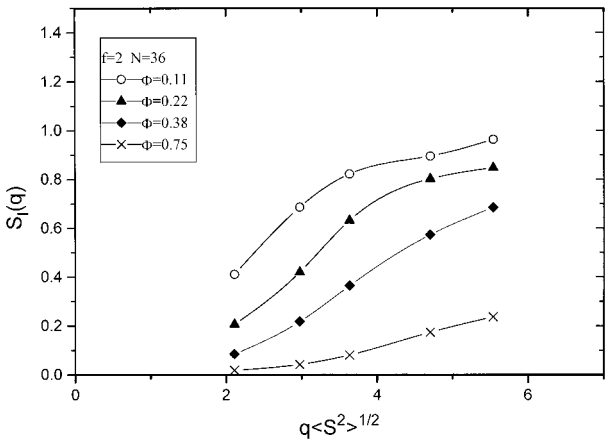

Figure 6. $S_I(q)$ vs $q\langle S^2\rangle^{1/2}$ for systems of linear chains and different concentrations. $\langle S^2\rangle$ corresponds to the result obtained with a single linear chain.

obtained from

$$S(q) = L^{-3}\langle[\sum_i^{L^3} f_i \cos(\mathbf{q}\cdot\mathbf{R}_i)]^2 + [\sum_i^{L^3} f_i \sin(\mathbf{q}\cdot\mathbf{R}_i)]^2\rangle \quad (10)$$

where $\mathbf{R}_i$ is the unit i position vector of site i. f_i is a contrast factor proportional to the difference between the local (solvent or polymer unit) refractive index of site i and the mean refractive index of the system. Practically we set[21]

$$f_i = -\Phi \quad (11a)$$

if site i is occupied by the solvent, and

$$f_i = 1 - \Phi \quad (11b)$$

if site i is occupied by a polymer unit.

Moreover, the components of $\mathbf{q}$ should comply with the following restrictions

$$q_k = (2\pi/\mathrm{L})n_k, \quad k \equiv x, y, z, \quad n_k = 1,2, \ldots \quad (12)$$

due to the presence of periodic boundary conditions. $S(q)$ should be distinguished from the form factor of an individual chain, P(q), whose study with the present model has been the object of a separate study.[22] The contribution to the total scattering intensity due to interactions between different star molecules can approximately be described in terms of a structure factor $S_I(q)$ so that

$$S(q) = \Phi N S_I(q) P(x) \quad (13)$$

We have evaluated $S_I(q)$ employing the individual form factors obtained for the dilute chains. (We showed in our previous work that $P(x)$ does not depend noticeably on the concentration, and we ignore here the moderate size chain contraction for increasing concentrations. This approximation is also used in the analysis of experimental data[1,23] and corresponds to a maximum error of 11% in the value of x for the present data. Therefore, it cannot affect to the qualitative aspect of the functions). In Figures 6−8 we present $S_I(q)$ for f = 2−4 at different concentrations. The functions have been calculated from data obtained in our previous work for linear chains[21] and also from the results obtained with the present simulations for the $f = 3$ and $f = 4$ star chains. We observe that, in general, $S_I(q)$ behaves as a monotonic function. Low increasing values of $S_I(q)$ for linear and star chains correspond to the presence of a plateau in the scattering function[24] for the systems with concentration beyond Φ^*. It should be considered that the presence of a peak with values of the structure function higher than 1 at $\Phi \cong \Phi^*$ is only experimentally observed for stars of considerably higher functionalities.[23,24] However, our curves systematically for star chains exhibit some roughness in the region $x^{1/2} = 2$ for $\Phi \cong 0.1-0.2$ which seems systematic and apparently exceeds the statistical noise. (Errors in our Monte Carlo data of the scattering data are smaller than 1%.) This effect is more noticeable for the $f = 4$ chains. Since according to eq 4, $\Phi^* \cong 0.15-0.20$ (see Table 1) for the considered chain lengths and the three types of chains (f = 2, 3, and 4), these irregularities can correspond to the onset of the ordering peak. This peak should be small for our stars with low numbers of branches. Therefore, it can be located below the asymptotic regime of the curves. Consequently, the present results may indicate some degree of ordering in the star semidilute solutions at $\Phi \cong \Phi^*$, though this ordering would be more clearly manifested in stars with a higher number of arms.

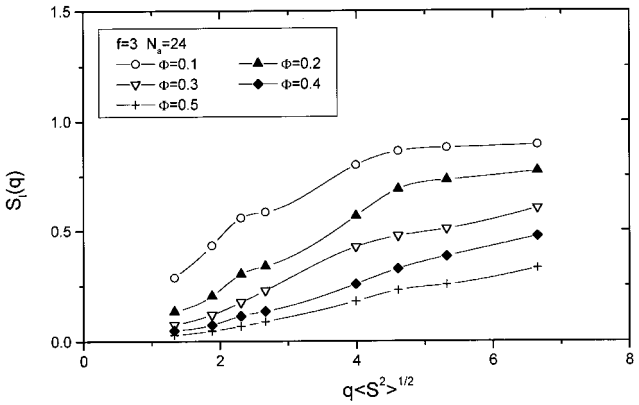

Figure 7. $S_I(q)$ vs $q\langle S^2\rangle^{1/2}$ for systems of star chains with f = 3 and different concentrations. $\langle S^2\rangle$ corresponds to the result obtained with a single star chain with $f = 3$.

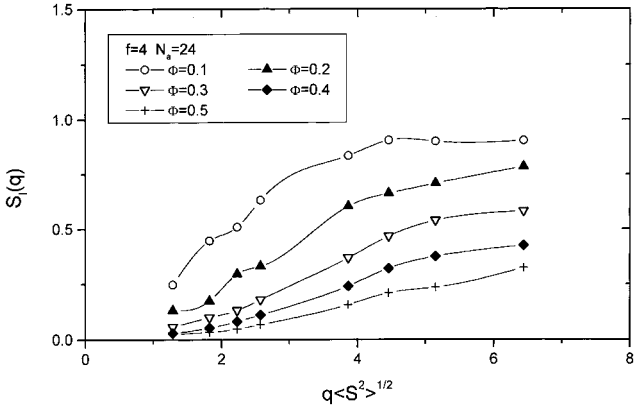

Figure 8. $S_I(q)$ vs $q\langle S^2\rangle^{1/2}$ for systems of stars chains with f = 4 and different concentrations. $\langle S^2\rangle$ corresponds to the result obtained with a single star chain with $f = 4$.

(c) Rouse Modes. The time−correlation functions corresponding to different Rouse modes can be computed as

$$C_k(t) = \langle \mathbf{u}_k(t)\cdot\mathbf{u}_k(t+\tau)\rangle_\tau \quad (14)$$

Table 5. Fitted Exponents $-a_k$ for the τ_k vs k Dependence[a]

f	single chain	$\Phi = 0.1$	$\Phi = 0.2$	$\Phi = 0.3$
3	2.16	2.10	2.11	1.95
4	2.19	2.09	2.05	2.07

[a] The log−log fits of the long chain limit extrapolations of τ_k/τ_1 vs k. $k = 1-4$.

Table 6. Fitted Exponents a_N for the τ_k vs N Dependence

f	k	single chain	$\Phi = 0.1$	$\Phi = 0.2$	$\Phi = 0.3$
3	1	2.10	2.15	2.12	1.92
	2	1.97	2.03	2.04	1.86
	3	2.04	2.14	2.11	2.00
	4	2.03	2.13	2.04	1.95
4	1	2.04	2.06	2.08	2.09
	2	1.93	1.86	1.99	2.04
	3	1.98	1.90	2.03	2.07
	4	1.95	2.03	2.09	1.97

where

$$\mathbf{u}(t) = \mathbf{Q}^{-1}\mathbf{R}(t) \tag{15}$$

R(t) is a column containing the chain different unit positions at time t and **Q** is the $N \times N$ transformation matrix, whose columns are the eigenvectors of the Rouse connectivity matrix **A**, as defined in the Zimm and Kilb theory.[25] (The particular form of this matrix depends on f). It should be considered that, according to this scheme, the chain exhibits $(f - 1)$-fold degenerate odd normal modes, with nondegenerate even normal modes. Both eigenvalues and eigenvectors can easily be obtained by numerical diagonalization of **A**. Hydrodynamic interactions, surely important in dilute conditions,[26] cannot be reproduced by our dynamic Monte Carlo algorithm and are, therefore, consistently ignored in our determination of the normal modes. (In any case, the normal modes are only modestly affected by the presence of hydrodynamic interactions.)

Our numerical time−correlation functions can be reasonably fitted to single-exponential functions of the type[26]

$$C_k(t) = A_k e^{-t/\tau_k} \tag{16}$$

obtaining this way numerical values for the relaxation times τ_k for the first four different normal modes, $k = 1-4$. We have performed long chain limit extrapolations of the ratios τ_k/τ_1. The log−log fits of these extrapolated ratios vs k have yielded the negative slopes $-a_k$ contained in Table 5 for $f = 3$ and $f = 4$ and different concentrations. It is observed that practically all these values of $-a_k$ vary as $1 + 2\nu_N$ between the values 2 and $1 + 2\nu \cong 2.18$, values that correspond to the predictions of the Rouse theory without and with excluded volume interactions. Moreover, the slopes show the general trend of decreasing for increasing concentrations, i.e., they tend to diminish when the excluded volume interactions are screened out. Also, we have performed log−log fits of τ_k vs N for $N_a = 12-100$. The slopes of these fits, a_N, have yielded the exponents contained in Table 6. The theoretical exponent expected from the Rouse theory is also $1 + 2\nu$ for the dilute case, though we expect an increase of a_N, due to the strong decrease of the chain translational diffusion coefficient with the chain length for nondilute systems.[26] (The slopes in these cases are expected to correspond to $-d_N + 2\nu_N$,

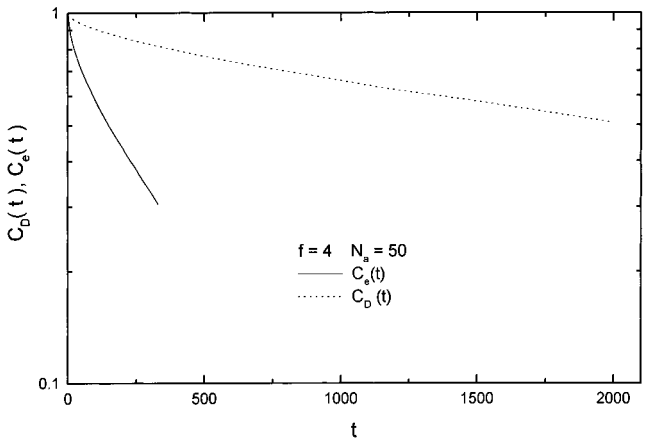

Figure 9. Semilogarithmic plots of $C_e(t)$ and $C_D(t)$ vs t for an illustrative case.

where d_N is the exponent of the variation of the translational diffusion coefficient with N for the given concentration. The Rouse theory predicts $d_N = -1$ for dilute conditions without hydrodynamic interactions, while $d_N = -2$ according to the tube model for completely entangled systems). However, our numerical values are generally slightly smaller than the absolute values of those obtained for the k dependence. We believe that these differences in the dilute solutions are due to finite size effects associated to the presence of the core region. This is more clearly shown in the case $f = 4$. Moreover, these results show higher nonsystematic oscillations than the a_k values, and a clear tendency of their dependence with Φ cannot be observed. Previously obtained values for linear chains, however, exhibited a significant increase of a_N for higher concentrations.[6] It should be considered than the presence of cores partially inhibits the chains mutual interpenetration of star chains so that, in the semidilute region, the decrease of ν_N for higher concentrations due to the screening out of excluded volume can partially compensate the increase of $-d_N$ caused by entanglement effects. Despite these effects, our algorithm shows the essential features associated with the Rouse dynamics. This serves, in our opinion, as an adequate verification of its capability to reproduce dynamic properties.

(d) Elastic and Rotational Modes. Intramolecular interactions in the star core are always present in dilute conditions. Therefore, some dynamic motions cannot be easily described in terms of the normal modes. Thus, we consider the elastic mode corresponding to fluctuations in the global size of the star that can be obtained as

$$C_e(t) = \frac{\langle R_C(\tau)R_C(\tau + t)\rangle_\tau - \langle R_C\rangle^2}{\langle R_C{}^2\rangle - \langle R_C\rangle^2} \tag{17}$$

where R_C is the center-to-end distance of any branch. In Figure 9 we present the logarithmic plot of $C_e(t)$ for an illustrative case. It is shown that, after an initial curvature at very short times, a linear behavior governed by a single relaxation time can be easily distinguished. Then, if one disregards the initial part of the curves, a numerical fit of the time-correlation functions to a single exponential, similar to eq 16, yields the elastic relaxation times, τ_e. The scaling theory predicts that this relaxation time should vary with the number

Table 7. Results for τ_e and τ_D

		N_a				
	f	12	16	24	32	50
$\tau_e \times 10^{-2}$	3	0.152 ± 0.004	0.242 ± 0.003	0.590 ± 0.003	1.18 ± 0.01	3.23 ± 0.03
	4	0.21 ± 0.01	0.269 ± 0.007	0.68 ± 0.02	1.13 ± 0.01	3.19 ± 0.04
$\tau_D \times 10^{-3}$	3	0.164 ± 0.003	0.318 ± 0.003	0.663 ± 0.003	1.19 ± 0.01	3.35 ± 0.01
	4	0.257 ± 0.001	0.403 ± 0.002	0.994 ± 0.003	1.72 ± 0.01	4.03 ± 0.02

of units and the star functionality according to eq 5. Our results for τ_e are included in Table 7, together with the errors evaluated by the numerical fitting procedure. The log−log fits of these results vs N_a yields slopes of 2.17 and 1.94 for $f = 3$ and $f = 4$, respectively. The former value is in excellent agreement with the expected $1 + 2\nu$ theoretical behavior, but the result for $f = 4$ is clearly smaller that the theory prediction (similar differences with theory were discussed above for the relaxation times of normal modes in the case $f = 4$). Although only two functionalities are explored, it is clear that a weak dependence on f is obtained for different chain lengths, in good agreement with theory. Similar conclusions have been obtained in previous numerical simulations.[12−14]

The time correlation functions of the center-to-end distance

$$C_D(t) = \frac{\langle \mathbf{R}_C(\tau)\cdot\mathbf{R}_C(\tau + t)\rangle_\tau}{\langle R_C^{\,2}\rangle} \qquad (18)$$

are similarly decaying curves (see Figure 9) which allow for the definition of the rotational relaxation time, τ_D. This is the time required for the star to rotate or to translate a distance similar to its size. Consequently, it should not be affected by core effects. The scaling theory prediction for the corresponding relaxation time τ_D is given by eq 6.

In Table 7, we also include our numerical values of these relaxation times. It can be noted that they are about a decade larger than the elastic times. Previous simulations could not characterize this mode as a single exponential.[1,12] The log−log fits of τ_e vs N yield the slopes 2.11 for $f = 3$ and 1.96 for $f = 4$, which are close to the previously discussed results obtained from the τ_e data. The log−log slopes of the variation of τ_e with f (only two data points for each value of N) yield a mean value 1.1 ± 0.2. This is clearly smaller than the theoretical value 1.41, which is based in the scaling theory and, therefore, it can only hold for high functionalities. Nevertheless, the present numerical values are consistent with the significantly higher dependence on f that can be expected for the rotational relaxation times in comparison with the weak dependence associated to the elastic relaxation times.

Acknowledgment. This research was supported by Grant PB95-0384 of the DGICYT (Spain). L.A.M. acknowledges a fellowship from the MEC (Subprogram PFI).

References and Notes

(1) Grest, G. S.; Fetters, L. J.; Huang, J. S.; Richter, D. *Adv. Chem. Phys.* **1996**, *94*, 67.
(2) Daoud, M.; Cotton, J. P. *J. Phys.* **1982**, *43*, 531.
(3) Douglas, J. F.; Roovers, J.; Freed, K. F. *Macromolecules* **1990**, *23*, 4168.
(4) Freire, J. J. *Adv. Polym. Sci.* **1999**, *143*, in press.
(5) Binder, K. In *Monte Carlo and Molecular Dynamics Simulations in Polymer*; Binder, K., Ed.; Oxford University: New York, 1995.
(6) López Rodriguez, A.; Rey, A.; Freire J. J. *Macromolecules* **1992**, *25*, 3266.
(7) Sikorsky, A. *Makromol. Chem. Theory Sim.* **1993**, *2*, 309.
(8) Sikorski, A.; Romiszowski, P. *J. Chem. Phys.* **1996**, *104*, 8703.
(9) de Gennes, P.-G. *Scaling Concepts in Polymer Physics*; Cornell: Ithaca, NY, 1979.
(10) Flory, P. J. *Principles of Polymer Chemistry*; Cornell: Ithaca, NY, 1953.
(11) Witten T. A.; Pincus P. *Macromolecules* **1986**, *19*, 2509.
(12) Su S.-J.; Denny, M. S.; Kovac, J. *Macromolecules* **1991**, *24*, 917.
(13) Ohno, K.; Schulz, M.; Binder, K.; Frish H. C. *J. Chem. Phys.* **1994**, *101*, 4452.
(14) Grest, G. S. *Macromolecules* **1994**, *27*, 3493.
(15) López Rodriguez, A.; Freire, J. J. *Macromolecules* **1991**, *24*, 3578.
(16) Batoulis, J.; Kremer, K. *Macromolecules* **1989**, *22*, 4277.
(17) Wei, G.; Eichinger, B. E. *J. Chem. Phys.* **1990**, *93*, 1430.
(18) Bishop, M.; Clarke, J. H. R.; Rey, A.; Freire, J. J. *J. Chem.* Phys. **1991**, *94*, 4009.
(19) Forni, A.; Ganazzoli, F.; Vacatello, M. *Macromolecules* **1997**, *30*, 4737.
(20) Zifferer, G. *Macromol. Theory Simul.* **1994**, *3*, 163.
(21) López Rodriguez, A.; Freire, J. J.; Horta, A. *J. Phys. Chem.* **1992**, *96*, 3954.
(22) Molina, L. A.; Rey, A.; Freire, J. J. *Comput. Theor. Polym. Sci.* **1997**, *7*, 243.
(23) Richter, D.; Jucknischke, O.; Willner, L.; Fetters, L. J., Lin, M.; Huang, J. S.; Roovers, J.; Toporowski, P. M.; Zhou, L. L. *J. Phys. IV Suppl.* **1993**, *3*, 3.
(24) Roovers, J.; Toporowski, P. M.; Douglas J. *Macromolecules* **1995**, *28*, 7064.
(25) Zimm, B. H.; Kilb, R. W. *J. Polym. Sci.* **1959**, *37*, 19.
(26) Doi, M.; Edwards, S. F. *The Theory of Polymer Dynamics*; Clarendon: Oxford, 1987.

MA980722Z